Performance limitations of GaAs/AlGaAs infrared superlattices

M. A. Kinch
Texas Instruments Incorporated, Dallas, Texas 75265

A. Yariv
California Institute of Technology, Department of Applied Physics, Pasadena, California 91125

(Received 17 May 1989; accepted for publication 13 September 1989)

The performance of the GaAs/AlGaAs superlattice as an infrared detecting material is modeled as a function of temperature for two cutoff wavelengths, namely, 8.3 and 10.0 μm. The results are compared with HgCdTe, the present industry standard material for infrared systems. The limiting performance of the GaAs/AlGaAs materials system is found to be orders of magnitude below that of HgCdTe for any specific cutoff wavelength and operating temperature.

The concept of infrared (IR) photodetection by intersubband absorption in superlattices first proposed by Smith *et al.*[1] has recently become the subject of extensive investigation[2] utilizing the GaAs/AlGaAs system, and strong claims have been made regarding the performance of this IR materials system relative to that of HgCdTe. It is the purpose of this letter to meaningfully compare the ultimate performance of these two materials systems with a view to their potential application in infrared systems. To this end a quantitative analysis is carried out of a $\lambda_c = 8.3$ μm superlattice, and this is compared both to the published data and to a HgCdTe photoconductor operating at the same cutoff wavelength. These arguments are then extended to the more relevant range for IR systems, namely, $\lambda_c = 10$–12 μm.

The GaAs/AlGaAs multiquantum well detector is a majority-carrier device, and as such the noise is determined by the variance in the density of majority carriers[3,4] within the device, namely, $\langle \Delta n^2 \rangle = n = n_t + n_\phi$, where n_t is the density of thermally generated carriers and n_ϕ the density of photon-generated carriers. The photon-generated carrier density consists of two components, due to signal (ϕ_s) and background flux (ϕ_B), and in the 8–12 μm spectral region is dominated by the background optical flux component $n_{\phi B}$. The ultimate in IR system performance is achieved when $n_{\phi B} > n_t$, as the noise is then dominated by the incident background flux, and background-limited performance (BLIP) is achieved.

The thermally generated carrier density for the multiquantum well structure is obtained from a consideration of the density of states in the associated bandstructure of a single quantum well. The geometry of the structure considered consists of 50 GaAs quantum wells of width 40 Å, with $Al_xGa_{1-x}As$ barriers ($x = 0.31$) of thickness 300 Å and height 250 mV. An envelope function approximation[5] calculation for this structure yields the energy-level diagram shown in Fig. 1. The first subband lies approximately 100 mV above the GaAs conduction-band edge, and the second subband lies approximately 3 mV above the continuum edge of the barrier. The GaAs wells are doped at $n_0 = 2\times10^{18}$ to provide the necessary IR absorption coefficient for the structure. The Fermi level is calculated, to a good approximation, assuming an infinite barrier, so that for the two-dimensional density of states associated with the first subband E_1, we have

$$E_F = n_0 \Pi \hbar^2 d/m^*, \tag{1}$$

where d is the well width and m^* the effective mass. For $n_0 = 2\times10^{18}$ cm^{-3}, $d = 40$ Å, and $m^* = 0.067m_0$, we have $E_F = 28.7$ mV. Using the model of Fig. 1 we treat the continuum as a wide quantum well of width L equal to the mean well spacing, and the two-dimensional density of states is then (assuming only one state, $n = 1$, is confined in the deep well)

$$\rho_{2D}(E) = \frac{m^*}{\Pi\hbar^2}\left\{1 + \mathrm{Int}\left[L\left(\frac{2m^*(E-V)}{\hbar^2\Pi^2}\right)^{1/2}\right]\right\}, \tag{2}$$

where $\mathrm{Int}(x)$ = largest integer $< x$. The corresponding volumetric density (electrons/cm^3 – eV) is ρ_{2D}/L. We note that for $L[2m^*(E-V)/\hbar^2\Pi^2]^{1/2} \gg 1$, the volumetric density is $\rho_{2D}/L \to (2m^*/\hbar^2)^{3/2}(E-V)^{1/2}/2\Pi^2$, which is the bulk value.

The density of thermally generated carriers above the barrier $E = V$ is thus

$$n_t = \frac{m^*}{\Pi\hbar^2 L}\int_V^\infty \left\{1 + \mathrm{Int}\left[L\left(\frac{2m^*(E-V)}{\hbar^2\Pi^2}\right)^{1/2}\right]\right\} \times \frac{dE}{e^{(E-E_F)/kT}+1} \tag{3}$$

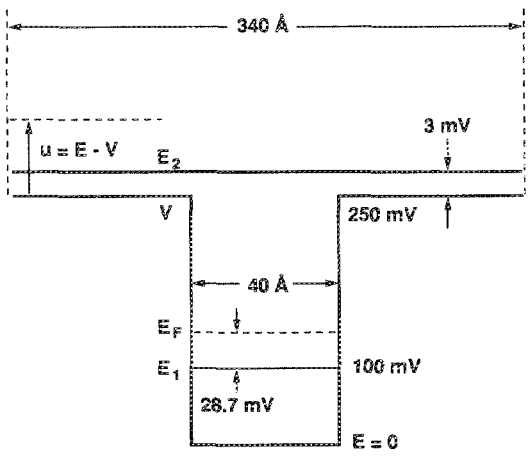

FIG. 1. 8.3 μm IR quantum well structure.

 0003-6951/89/462093-03$01.00

$$\approx \frac{m^* e^{(V-E_F)/kT}}{\Pi\hbar^2 L}\int_0^\infty \left\{1+\mathrm{Int}\left[L\left(\frac{2m^*u}{\hbar^2\Pi^2}\right)^{1/2}\right]\right\} \times e^{-u/kt}\,du. \tag{4}$$

For the parameters of Fig. 1, $\mathrm{Int}[L\sqrt{(2m^*u/\hbar^2\Pi^2)}]=0$ for $u<3$ mV, and $=1$ for $u>6$ mV. At $u=6$ mV, $\exp(-u/kT)\sim\exp(-1)$ at 77 K. To first order we can neglect the Int( ) term in Eq. (4), obtaining

$$n_t = (m^*kT/\Pi\hbar^2 L)e^{-(V-E_F)/kT}, \tag{5}$$

noting that this will represent a slight underestimate of n_t. This approximation is tantamount to assuming that all thermal carriers are generated by the first electron subband of the quantum well.

Combining Eqs. (1) and (5) we have

$$n_t = n_0\left(\frac{kT}{E_F}\right)\frac{d}{L}e^{-(V-E_F)/kT}. \tag{6}$$

The background-generated carrier density is given by, for an incident angle of 45°,

$$n_{\phi_B} = \eta\phi_B\tau/\sqrt{2}t, \tag{7}$$

where τ represents the effective lifetime of excess carriers, t, the device thickness, and η the device quantum efficiency. The measured[2] flattening of responsivity with bias voltage for $V_b>4$ V indicates that τ is then $\sim\tau_d/2=t/2v$, where τ_d is the transit time of a hot electron across the device structure, and v its limiting velocity, which for GaAs/AlGaAs will be $\sim10^7$ cm/s. Thus, $\tau\sim8.5\times10^{-12}$ s. This hot-electron lifetime value is considerably larger than that found for absorption in GaAs quantum wells between two bound states,[6] where $\tau\sim1$–2×10^{-13} s. This could possibly be attributed to both the unbound nature of the first excited subband, and to the larger AlGaAs barrier widths employed. The hot electron thus spends a large fraction of its lifetime in the barrier region, where it cannot lose its excess energy. It should be pointed out that these observed values are somewhat lower than would be predicted by hot-electron theory,[7,8] assuming energy loss simply by electron-phonon interactions. This is possibly due to the role played by electron-electron scattering. The quantum efficiency is determined from the measured responsivity in the sweepout mode, namely, $\eta q/(2\sqrt{2}h\nu)$, where a photoconductive gain of 1/2 and a 45° angle of incidence have been assumed. The measured value[2] for unpolarized light is 0.42 A/W, giving $\eta\sim17.5\%$. Assuming two passes of IR radiation through the superlattice at an angle of 45°, this corresponds to an absorption coefficient for unpolarized light, $\alpha\sim750$ cm^{-1}, in reasonable agreement with measured values[2] for this device at 8.3 μm.

From Eqs. (6) and (7) the BLIP condition is achieved when $\eta\phi_B\tau/t\sqrt{2}>n_t$, or rearranging we have BLIP when the 45° incident background rate of carriers, $\eta\phi_B/\sqrt{2}>n_t t/\tau$, the thermal generation rate of carriers in the detector. The thermal generation rate can be viewed as the rate at which any departure from equilibrium in the device is accommodated. A calculation of the thermal generation current, $J_t(=n_t tq/\tau)$, in the 8.3 μm GaAs-AlGaAs superlattice as a function of temperature is shown in Fig. 2, assuming $\tau=8.5$ ps, $t=1.7$ μm, $d=40$ Å, $L=340$ Å, and $n_0=2\times10^{18}$ cm^{-3}. The current is normalized by the effective material quantum efficiency ($=0.175/\sqrt{2}$) so as to facilitate comparison with other materials systems. Plotted on the right-hand axis is the equivalent incident photon flux. This plot immediately gives the required minimum temperature of operation such that $n_t\leqslant n_{\phi B}$. For example, at a typical system background flux of 10^{16} photons/cm^2 s, the required temperature of operation for the 8.3 μm GaAs-AlGaAs superlattice is <69 K to achieve the BLIP condition.

Operation at 8.3 μm is not particularly meaningful for practical IR systems, and a cutoff wavelength of 10.0 μm is more relevant. The preceding calculation is extended to consider this case. The quantum well width is changed to 30 Å, and the remaining parameters assumed the same. This will yield an intersubband transition energy ~0.124 eV. The calculated thermal generation rate (and hence current) for this case is also shown in Fig. 2 as a function of temperature. BLIP performance for 10 μm wavelengths in a 10^{16} cm^2 s environment requires operating temperatures <58 K.

Similar arguments can be readily applied to HgCdTe operating at the same cutoff wavelengths. HgCdTe devices are dominated by minority-carrier statistics, so for n-type HgCdTe the BLIP condition becomes $p_n t/\tau_p<\eta\phi_B$, where $p_n=n_i^2/n_0$, n_i being the intrinsic carrier concentration. In good quality HgCdTe, the minority-carrier lifetime τ_p is limited by Auger recombination[9] and is given by

$$\tau_p = 2\tau_{\mathrm{Ai}}n_i^2/n_0^2, \tag{8}$$

where τ_{Ai} is the intrinsic Auger lifetime. Thus, the thermal generation rate of minority carriers in good quality HgCdTe is given by

$$p_n t/\tau = n_0 t/2\tau_{\mathrm{Ai}}. \tag{9}$$

τ_{Ai} has been measured[9] for a variety of HgCdTe composi-

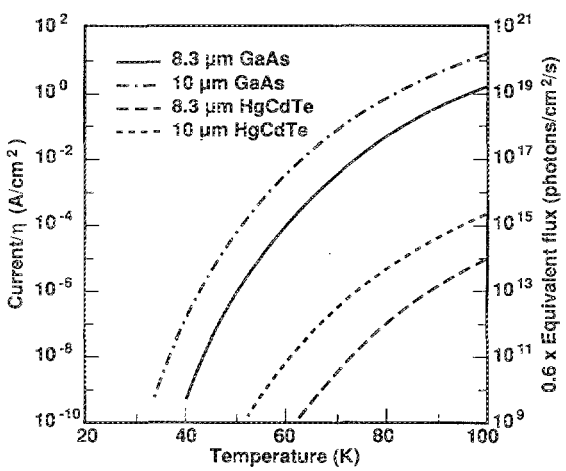

FIG. 2. Thermal generation current vs temperature for GaAs/AlGaAs IR superlattices and HgCdTe alloys at $\lambda_c=8.3$ and 10 μm. The assumed effective quantum efficiencies are $\eta=0.125$ and 0.7 for GaAs/AlGaAs and HgCdTe, respectively.

tions, is in reasonable agreement with theory,[10] and is given approximately by

$$\tau_{Ai} = [8.3\times10^{13}E_g^{1/2}/(kT)^{3/2}]\exp(E_g/kT), \quad (10)$$

where a value for the overlap integral $|F_1F_2|^2 = 0.25$ has been assumed to fit the experimental data.

The minority-carrier generation current given by Eqs. (9) and (10) is shown in Fig. 2 as a function of temperature for both 8.3 and 10 μm cutoff wavelengths. A quantum efficiency of 0.7 has been assumed to normalize the thermal current axis. It is readily apparent from Fig. 2 that the thermal generation rate at any specific temperature and cutoff wavelength is approximately five orders of magnitude smaller than for the corresponding GaAs-AlGaAs superlattice. This translates into a cooling requirement of an additional 50 K for GaAs-AlGaAs to achieve the same performance as HgCdTe. The dominant factor favoring HgCdTe in this comparison is the excess carrier lifetime, which for n-HgCdTe is $>10^{-6}$ s at 80 K, compared to 8.5×10^{-12} s for the IR superlattice.

It should be pointed out that the GaAs/AlGaAs superlattices considered above are not theoretically optimized structures. Some benefit can be gained by trading off device thickness and doping concentration, such that a high overall quantum efficiency is maintained but with a subsequent decrease in E_F, and hence n_t. Some enhancement of carrier lifetime can be achieved by widening the barrier layers, but there are limits. For the quantum well geometries considered the Int$[L(2m^*u/\hbar^2\Pi^2)^{1/2}]$ term in Eq. (4) will no longer be negligible for values of $L>500$ Å. Thus, any increase in τ would be offset by an increase in n_t, essentially due to thermally generated carriers in the AlGaAs barrier region. It is also not apparent that the photoconductive gain of this device must necessarily be limited to the value 1/2. The choice of GaAs contacts[2] generates Schottky barriers at the input and output of the superlattice. It would seem that a judicious choice of heavily doped $Al_xGa_{1-x}As$ of the appropriate x composition could generate ohmic contacts to the superlattice device. Hence photoconductive gain greater than unity could be achieved, provided the dielectric relaxation time ($=\rho\epsilon\epsilon_0$, where ρ is the resistivity and ϵ the dielectric constant) were fast enough for the operating conditions.

The thermal generation rate parameter can be used to directly estimate D^* if so desired. For a photoconductive detector, with radiation incident at an angle θ to the normal, the specific peak detectivity is given by $D^* = \eta(\tau\cos\theta/n_t t)^{1/2}/2h\nu$, where η represents the absorbing quantum efficiency, which for the GaAs-AlGaAs cases treated here was 17.5%. At 80 K the two superlattices considered here would exhibit maximum values of $D^*_\lambda(8.3\,\mu\text{m}) = 1.85\times10^{10}$ cm Hz$^{1/2}$ W^{-1}, and $D^*_\lambda(10.0\,\mu\text{m}) = 6.1\times10^{9}$ cm Hz$^{1/2}$ W^{-1}, compared to HgCdTe, with $D^*_\lambda(8.3\,\mu\text{m}) = 1.75\times10^{13}$ cm Hz$^{1/2}$ W^{-1}, and $D^*_\lambda(10.0\,\mu\text{m}) = 3.0\times10^{12}$ cm Hz$^{1/2}$ W^{-1}.

In summary, it is shown that the limiting performance of GaAs-AlGaAs IR superlattices is considerably below that which can be achieved with HgCdTe devices at any specific temperature and cutoff wavelength. Performance requirements of present day IR systems [operating in typical 10 μm flux environment of $(1\text{–}3)\times10^{16}$ photons/cm^2 s] would necessitate operation of GaAs-AlGaAs superlattices at temperatures below 60 K.

One of the authors (A.Y.) acknowledges the Material Research Council of the Defense Advanced Projects Agency and the Office of Naval Research for support of this work. The authors acknowledge fruitful discussions with Dr. T. C. McGill and Dr. H. Ehrenreich.

[1] J. S. Smith, L. C. Chiu, S. Margalit, A. Yariv, and A. Y. Cho, J. Vac. Sci. Technol. B **1**, 376 (1983).
[2] B. F. Levine, C. G. Bethea, G. Hasnain, J. Walker, and R. J. Malik, Appl. Phys. Lett. **53**, 2196 (1988).
[3] K. M. van Vliet, Proc. IRE **46**, 1004 (1958).
[4] D. Long, Infrared Phys. **7**, 169 (1967).
[5] G. Bastard, Phys. Rev. B **25**, 7584 (1982).
[6] B. F. Levine, K. K. Choi, C. G. Bethea, J. Walker, and R. J. Malik, Appl. Phys. Lett. **50**, 1092 (1987).
[7] R. Stratton, Proc. R. Soc. London A **246**, 406 (1957).
[8] B. K. Ridley, J. Phys. C **15**, 5899 (1982).
[9] M. A. Kinch, M. J. Brau, and A. Simmons, J. Appl. Phys. **44**, 1649 (1973).
[10] P. E. Petersen, J. Appl. Phys. **41**, 3465 (1970).